scientific reports

Check for updates

OPEN

Optimized PI controller-based hybrid model for adaptive energy management in photovoltaic integrated electric vehicle charging microgrids

Rathika Natarajan[1], Jaisiva Selvaraj[2], Shyam Daniel[3] & Tefera Mekonnen Azerefegn[4]✉

The demand for charging stations (CSs) has increased due to the rapid expansion of electric vehicles (EVs), which has led to higher peak loads and grid instability. Microgrids (MGs) can benefit from the integration of renewable energy sources (RES), but their intermittent nature requires clever and flexible energy management techniques. For a DC microgrid that includes photovoltaic (PV) generation, fuel cells, battery storage, and EV charging infrastructure, this research proposes an optimized PI-based hybrid energy management system. To achieve reliable power balancing under changing EV demand and fluctuating RES availability, the hybrid controller combines a fuzzy logic controller (FLC) with a Dwarf Mongoose-based Red Panda Optimization (RPO) algorithm for optimal proportional integral (PI) tuning. MATLAB/Simulink is used to model and validate the proposed method. The results show that enhanced renewable use, efficient converter management, and dynamic tariff adjustment considerably reduce operating costs and increase stability. During off-peak hours, charging costs drops to a minimum of 0.034 USD/kWh. Weekday and weekend average costs drop to 0.086 and 0.088 USD/kWh, respectively, representing reductions of 45.26% and 56.11%. Power balance is improved, and greenhouse gas emissions are reduced by up to 55.75% when renewable energy is used. In comparison to traditional techniques, the proposed optimized PI-based hybrid controller also exhibits better voltage regulation and faster convergence. These results demonstrate the hybrid adaptive EMS improves power stability, cost effectiveness, and renewable integration for DC microgrids that facilitate EV charging.

Keywords Renewable energy systems, Dwarf Mongoose-Based Red Panda Optimization, Microgrid, Electric vehicle, Charging station, Energy management system

Abbreviations

EVs	Electric vehicles
CSs	Charging stations
EMS	Energy management strategy
MG	Microgrid
RES	Renewable energy sources
PM	Power management
ICE	Internal combustion engine
EVCSs	EV charging stations
PI	Proportional integral
FLC	Fuzzy logic control
CCs	Charging costs

[1]Department of Electrical and Electronics Engineering, SKP Engineering College, Tiruvannamalai, Tamilnadu, India. [2]Department of Electrical and Electronics Engineering, Sri Krishna College of Engineering and Technology, Coimbatore, Tamilnadu, India. [3]Department of Electrical and Electronics Engineering, Rajalakshmi Engineering College, Chennai, Tamilnadu, India. [4]Faculty of Electrical and Computer Engineering, Jimma University, Jimma, Oromia, Ethiopia. ✉email: tefera.mekonnen@ju.edu.et

BCs	Boost converters
SSA	Sparrow Search Algorithm
PSO	Particle Swarm Optimization
PHEVs	Plug-In hybrid electric vehicles
MHS	Modified Harmony Search
PV	Photovoltaic
DNN	Deep neural networks
VSC	Voltage source converter
MPPT	Maximum power point tracking
ANN	Artificial neural networks
CSB	Charging station battery
SoC	State of charge
CEEMD	Complete ensemble empirical mode decomposition
FC	Fuel cell
RPO	Red Panda Optimization
DMO	Dwarf Mongoose Optimization
DMRPO	Dwarf Mongoose-Based Red Panda Optimization

Due to the rapid adoption of electric vehicles (EVs), the global automotive industry has seen a dramatic transformation in the past ten years[1]. This change has been facilitated by government incentives, consumer tax refunds, technological breakthroughs, and the pressing need to reduce greenhouse gas emissions[2]. To lower carbon emissions and foster green economic growth, governments everywhere are actively promoting sustainable transportation options[3]. Because of this, EV sales have surged substantially, spurred along by significant investments from high industrialist[4]. Shared mobility services, autonomous driving technology, logistics optimization, and improving personal mobility are currently the main drivers of developing business models[5]. Simultaneously, a number of nations have declared their intention to phase out internal combustion engine (ICE) vehicles within the next ten years, underscoring the vital need of creating a strong environment for EVs[6,7]. Nevertheless, the EV industry still faces several obstacles despite its quick growth, including range anxiety, expensive batteries, problems with charging standards, a lack of infrastructure for charging, and greater strain on power systems as a result of varying charging demands[8,9]. The combination of many charging connector types and the lack of standardized EV charging stations (EVCSs) further complicates widespread adoption[10]. Utility companies must install more Advanced EMS with charging stations as EV usage rises to control energy imbalances and peak load fluctuations[11,12]. It is now vital to integrate RES into the system to supply the growing requirement for electricity while cutting emissions[13]. However, real-time power management is a difficult issue due to the inherent uncertainty and intermittency of RES[14]. RES-powered MGs have become a viable option for efficiently managing energy supply and demand in EVCSs. MGs offer operational flexibility and reliable, resilient power delivery in both islanded and grid-connected modes. Still, the unpredictable properties have a significant impact on load balancing, storage use, and overall system stability because of the fluctuating nature of RES and EV charging trends[15]. Energy storage, renewable generation, and EV demand projections are therefore essential components of effective and cost-effective PM methods to prevent shortages or energy waste[16].

The unpredictable demand for EV charging, peak load fluctuations in microgrids, and the intermittent nature of renewable energy sources present difficulties for current energy management strategies. Traditional optimization methods can lack the flexibility required to adapt to changing operational conditions[17]. The temporal dependencies and nonlinear interconnections between EVCS demand, renewable generation, and storage systems are difficult for convolutional algorithms to capture, despite their effectiveness in spatial feature extraction and charging pattern identification. These restrictions make it difficult to forecast accurately and make decisions in real time, which leads to inefficiencies in power distribution and dependability. Therefore, sophisticated hybrid frameworks are needed to address these issues and provide economical, sustainable energy management.

The novelty of this work is its unique combination of bio-inspired optimization techniques and superior control strategies to enhance energy management in DC microgrids that support EV charging stations. It provides a hybrid architecture that makes use of a Fuzzy-PI controller in conjunction with the DMRPO algorithm to maximize power dispatch in the face of changing EV demand as well as the inherent unpredictabilities of renewable energy. By utilizing the social and foraging behaviours that the DMRPO simulates to better optimize the controller parameters, this approach outperforms conventional methods in terms of stability, reaction speed, and voltage regulation. Furthermore, incorporating a nature-inspired metaheuristic into a hybrid control system is a novel addition that offers a more robust and effective energy management solution that maximizes the use of renewable resources while preserving stable grid operation. This novel combination offers a feasible path for affordable and eco-friendly EV charging stations while addressing present issues in renewable microgrid management.

The primary contributions are highlighted below.

Contributions of the research:

The important contributions of the research are,

- Intelligent hybrid energy management is implemented to improve MG efficiency and enable efficient EVCS.
- Improving energy management in EVCSs by combining a proportional integral (PI) controller (PI-FLC) model with optimized fuzzy logic control using the Drawf Mongoose based Red Panda Optimization (DM-RPO) Algorithm.

- Integrating an optimized PI-based hybrid model to manage power inside the DC bus, ensuring stability in the face of load changes and uncertainties.

The paper is organized as follows: section "Literature review" presents the literature review, section "Proposed configuration of energy management in EVs" describes the proposed methodology for energy management in EVCS, section "Results and discussions:" explains the results and discussion and section "Conclusion" concludes the manuscript.

Literature review

Recent methods are used to examine the charging system of the suggested renewable energy-based RE system, and Table 1 summarizes their main drawbacks.

Karmaker, A.K., et al., [2023] examined issues with environmental and techno-economic aspects of electric vehicle charging system, highlighting the importance of a fuzzy logic algorithm. According to the study, the recommended methodology ensured a quick payback period for station owners by lowering Charging Costs (CCs) for weekdays and weekends as well as significantly reducing greenhouse gas emissions. According to the data, the recommended algorithm cuts energy expenses by a nominal level.

Hasani, R., et al., [2025] presented a clear 24-h scenario-based MG Energy Management System (MG-EMS) to lower operational costs and emissions in the face of uncertainty. In addition to flexible loads taking part in a Demand Response Program (DRP), the system incorporates PV units, Wind Turbine (WT) units, Combined Heat and Power (CHP), Power-to-Gas (P2G) storage, and an EV Parking Lot (EV-PL). Improved performance was demonstrated using a hybrid approach called the Hybrid Multiobjective Particle Swarm Optimization–Lightning Search approach (hMOPSO-LSA). The algorithm was applied to the MG-EMS case study after being verified using Deb–Thiele–Laumanns–Zitzler (DTLZ) benchmark functions.

Engelhardt, J., et al., [2022] examined an innovative EMS for hybrid fast charging system, employing a multi-battery architecture directly coupled to extra DC components without power converters. In comparison to basic droop control, the study demonstrated better self-sufficiency by introducing an advanced control with dynamic dead bands based on PV energy estimates. As a result, the suggested control achieves self-sufficiency to greater extent.

Mohamed, N., et al., [2021] investigated a PM algorithm for charging EVs on the move, utilizing a mix of wireless charging, PV generation, a battery system and a fuel cell. Boost Converters (BCs) for PV/FC and the boost-buck converter in the battery package were among the power converters for each energy source that were introduced in the study. To feed the battery series during periods of surplus energy availability, the novel method entailed connecting wireless charging, FC, and PV models in parallel via a DC/DC converter. For all aspect, mathematical models and matching PM loops were developed, demonstrating the research's important contribution. The battery's state of charge was found to be in feasible and optimum level.

Mohan, H.M. et al., [2023] investigated a hybrid optimization technique employing the Fuzzy-Sparrow Search Algorithm (SSA) for effective EMS in DC MGs with RES and battery storage. According to simulation data, the suggested SSA performed better in terms of stability and convergence rate than Particle Swarm Optimization (PSO). The Fuzzy-SSA displayed increased reaction characteristics, optimizing PM and minimizing electricity bills annually evaluated to PSO. The algorithm's contribution to economical PM for expanding EV charging infrastructure is highlighted in the report. Simulation results show that algorithm design in DC microgrids lowers annual electricity expenditures by at a better rate.

AL-Dhaifallah, M., et al., [2021] assessed the impact of charging plug-in hybrid electric vehicles (PHEVs) on the optimal operation of microgrids. To examine the behaviour of PHEVs, three alternative charging patterns comprising of uncontrolled, controlled and smart charging techniques are considered. Microgrid modeling energy management also considers prediction error in PHEVs, loads, pricing, and output electricity from renewable sources. To cope with the optimal scheduling of microgrid considering uncertainty, a modified harmony search (MHS) algorithm is utilized. The suggested system is validated using simulations and without the PHEV charging impacts.

Koca, Y.B., [2025] focused on modelling and regulating hybrid Photovoltaic (PV) and wind energy systems for EV battery charging stations. A load shedding system based on Deep Neural Networks (DNN) has been created. The integration of this mechanism with the grid through a voltage source converter (VSC) has been studied. The work stresses the integration of a DNN-based controller and maximum power point tracking (MPPT) method. The suggested system intends to reduce energy expenditures and optimize the load on the grid by boosting the usage of renewable energy sources. This unique solution has been created to address load balancing and stability difficulties in existing energy management systems. The research's main objectives are to maximize energy demand management and guarantee more effective use of renewable energy sources. Simulations conducted under various operational settings have tested the ability of the suggested DNN controller to manage loads dynamically according to three priority levels.

Sathyan, S., et al., [2024] introduced an EMS based on Artificial Neural Networks (ANN) used for the financial management of a PV-powered EVCS that includes battery backup and Vehicle to Grid (V2G) functionality. The Charging Station Battery (CSB) and Parking Lot EVs (PLV) support the efficient functioning of the EVCS and enhance its reliability by serving as a backup supply during independent mode, charging during off-peak hours and discharging during peak hours. The suggested approach lowers the operating costs of the PV-powered EVCS while guaranteeing that an appropriate power equilibrium is sustained among its different elements: PV, EV, CSB, the PLV prepared for V2G operation, and the grid. This approach utilizes real-time data, including the connection status of the EV and PLV, the State of Charge (SoC) for the EV, CSB, and PLV, available PV power, and Time of Use (ToU) tariff to intelligently allocate resources.

Authors []	Methods	Focus	Advantages	Limitations
Karmaker, A.K., et al.[18],	Fuzzy Logic Algorithm in EVCS	Techno-economic & environmental optimization	Reduces charging costs,Ensures quick payback Lowers greenhouse gas emissions	Limited to specific scenarios, Real- time grid constraints not addressed
Hasani, R., et al.[19]	hMOPSO-LSA	Energy management for smart MG EVCS	Hybrid structure improves multiobjective optimization performance, Achieves better convergence	Parameter tuning for hybrid algorithms are challenging
Engelhardt, J., et al.[20]	Hybrid Fast CSs with Multi-Battery Design	Hybrid fast- charging station autonomy	Improves system self-sufficiency, Outperforms basic droop control	No cost analysis, Hardware implementation challenges
Mohamed, N., et al.[21]	PM for Charging EVs on the Move	On-the-move EV charging	Efficient power coordination among sources, Provides flexible hybrid energy support	Very high system complexity, Requires multiple integrated energy sources
Mohan, H.M. et al.[22]	Hybrid Optimization with Fuzzy-SSA for DC MGs	EMS optimization in DC microgrids	Better stability and convergence, Reduces operating cost	Limited real-world testing, Performance under extreme loads not evaluated
AL-Dhaifallah[23]	Modified Harmony Search Algorithm	Microgrid scheduling with PHEV charging patterns	Manages uncertainty effectively, Improves microgrid operation with smart charging	Does not fully capture user charging behaviour, Scalability limitations
Koca, Y.B., et al.[24]	Hybrid PV–wind system with DNN-based load shedding, MPPT, VSC	Renewable-based EV charging with load balancing	Improves stability, optimizes renewable use, lowers costs	Requires large dataset and training for DNN
Sathyan, S., et al.[25]	ANN-based EMS with PV, battery & V2G	Financial and operational optimization of EVCS	Lowers operational cost, Ensures efficient power allocation, Improves system reliability using V2G and battery backup	Requires accurate real-time inputs, V2G participation is uncertain
Shen, Y., et al.[26]	Fuzzy logic with CEEMD	Battery–ultracapacitor energy split to reduce aging	Improves battery health, Maintains better SOC balance	No economic analysis , Limited to specific battery configurations
Kamel, O.M., et al.[27],	EV-assisted microgrid control with STATCOM support	Performance enhancement of islanded microgrids	Enhanced voltage stability, improved power quality	Higher system cost, limited focus on renewable uncertainty
Kamel, O.M., et al.[28],	Damping control techniques for DFIG-based wind farms	Oscillation damping in interconnected power systems	Effective suppression of low-frequency oscillations, improved system stability	Focused only on wind-integrated systems, not suitable for hybrid MGs,
Makram Kamel, O., et al.[39],	Novel FLC and JAYA-based optimal control	Energy management of isolated DC/AC microgrids under uncertainties	Improved voltage regulation and adaptive fuel consumption	High computational complexity, increased controller design effort

Table 1. Limitations of existing approaches.

Shen, Y., et al., [2023] presented a fuzzy logic energy management strategy for EVs that slows down battery aging by using Complete Ensemble Empirical Mode Decomposition (CEEMD). For power requirements, batteries and ultracapacitors contain distinct low- and high-frequency components, and a fuzzy controller maintains their charge levels. According to tests conducted battery capacity degradation is decreased by 6.72%, 8.33%, and 8.38%, respectively, due to decreased discharge current and enhanced SOC balance.

Makram Kamel, O., et al., [2023] examined a DC/AC microgrid functions in unpredictable operating environments. While the FC and BC help maintain MG stability, the PV system was regarded as the main energy source. A variable AC load and an electric vehicle charging system are provided by the MG. Two strategies for control are created and assessed. Initially, a new FLC was created to offer an EMS while taking conversion energy systems' uncertainties into account. A JAYA-based optimal control strategy was also used. The suggested EMS controls the charging of Li-ion batteries, keeps the load bus voltage steady, and controls FC fuel use. A PI controller tuned using the Ziegler–Nichols approach was used to compare the performance of the suggested controllers under partial PV shading.

Kamel, O.M., et al., [2023] presented a hybrid islanded MG model that integrates both EVs and STATCOM while taking into account a number of sustainable energy sources, including wind and PV. Residential system loads are present. With the use of EVs and DSTATCOM, this research aims to achieve frequency and voltage stability under challenging operating conditions. The performance of the suggested MG was examined for eight hours of operation, which corresponds to the higher load demand period. Fixed power factors are typically used by intermittent renewable energy systems, such as solar PV and wind. Also, rather than creating energy, these devices take in reactive electricity from the grid utility. Therefore, these new systems voltage regulation was supported by reactive power based on power electronics. The stability performance is enhanced using DSTATCOM as one of the most effective FACTS devices.

Kamel, O.M., et al., [2020] presented a various control strategies for wind farms based on doubly fed induction generators (DFIG) with the appropriate POD. To improve system oscillation damping, a damping control loop (DCL) was added to the DFIG back-to-back converter control circuit. DCL and the traditional power system stabilizer share a similar primary purpose. However, in order to maintain wind farms following grid code requirements and support system performance during congestion, external regulating devices like STATCOM are needed. Power system stabilizer (PSS), an incorporated component in the thermal power plants' management circuit, was used to examine the system's dynamic performance. Using MATLAB/Simulink, a system dynamic performance was carried out.

An evaluation of the current research indicated in Table 1 identifies several study gaps that restrict its relevance to actual EV charging settings. Scalability is limited when RES variability and EV arrival uncertainty grow since many systems rely on idealized operating conditions and lack thorough validation under highly dynamic load profiles. While certain solutions (such DNN and data-driven methods) show strong results in isolated circumstances, real-time implementation is difficult due to their high computational cost or need for vast datasets. Furthermore, most of the research concentrates on either technical performance or economic optimization, failing to include both elements into a cohesive control structure. The literature discusses hybrid energy systems with many sources (PV, FC, battery), but their control approaches rarely address converter coordination, fast response needs, and stability under transient disturbances. Moreover, only few studies offer adaptive controller tuning that can react to unanticipated fluctuations and nonlinearities under microgrid settings. These limitations highlight the need for an EMS that is more reliable, flexible, and computationally effective. To improve stability, lower charging costs, and increase renewable use in the face of real-time operational uncertainty, the proposed optimized PI- based hybrid model combines intelligent controller tuning with fuzzy decision-making.

Proposed configuration of energy management in EVs

The proposed DC microgrid system under consideration comprises of an electric vehicle charger, a battery storage system, an energy system powered by fuel cells, and a photovoltaic solar system is depicted in Fig. 1. The solar PV system greatly reduces greenhouse gas emissions and electricity costs. PV is the best option for operating a self-sufficient grid. The energy of PV systems is dependent on temperature, irradiance, and voltage. Electrical devices called photovoltaic cells employ semiconducting components to generate power from solar rays. A boost converter connects the PV array to the DC bus. The greatest part of the solar curve can power a photovoltaic system by employing a booster converter that uses the MPPT (maximum power point tracking) technique[18]. It also maintains the power balance of the microgrid by storing or releasing excessive or insufficient electricity. The battery storage system is powered by a bidirectional converter that allows for both charging and discharging[38]. Energy flow optimization and general coordination are regulated by an optimized PI-based hybrid model energy management plan that assures the hybrid energy system's stability, reliability, and effective operation.

Modelling of photovoltaic system

Photovoltaic (PV) systems are a sustainable and renewable method of producing clean energy[35]. The main variables affecting PV system's output power are solar irradiation, cell temperature, and the placement of the PV array. The main components of the analogous PV model circuit are a diode D, internal shunt and series resistances R_{sh} and R_s, and a current source I_L whose magnitude is influenced by temperature and solar irradiation. Equation (1) presents the voltage-current VI characteristics.

$$I_{PV} = I_L - I_0 \left[\exp\left(\frac{q\left(V_{PV} + R_s I_{PV}\right)}{akT} - 1 \right) \right] - \frac{V_{PV} + R_s I_{PV}}{R_{sh}} \tag{1}$$

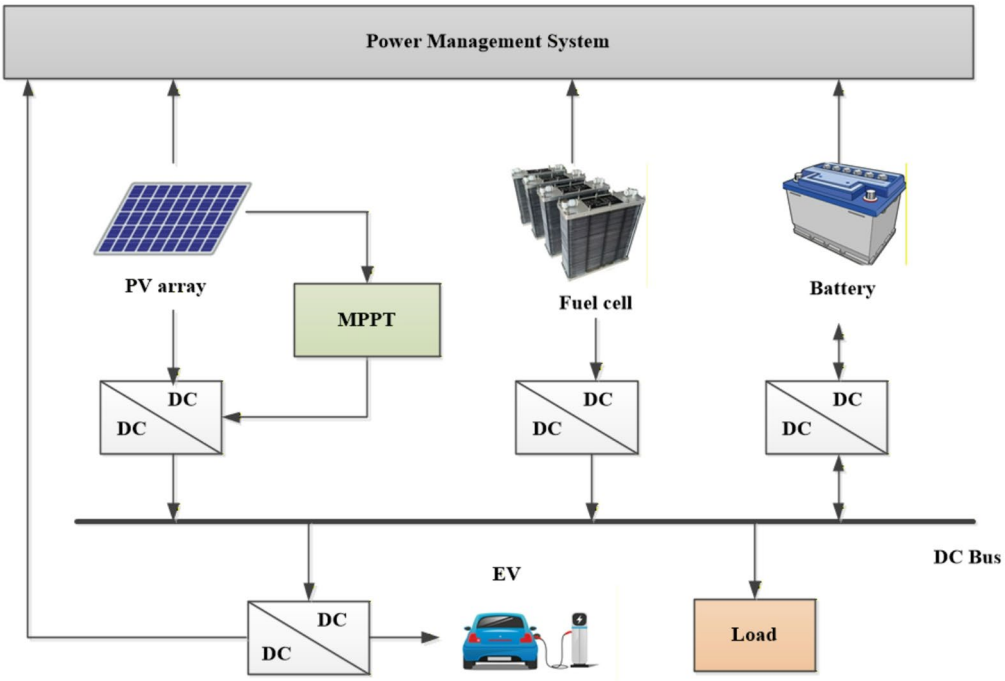

Fig. 1. A microgrid layout powered by sustainable energy.

where, I_{PV} represent the PV current, V_{PV} represent the each cell's voltage, I_0 represent the reverse saturation current of the diode, q represent the electron charge, a represent the p–n junction ideality factor, k represent the Boltzmann constant and T represent the temperature. The output of PV panels is greatly impacted by the intensity and distribution of solar radiation.

Modelling of fuel cell

Fuel cells are clean energy sources that use electrolyzers to transform chemical energy into DC electrical energy[36]. It functions similarly to a battery, but it doesn't require recharging and has additional benefits than a battery, including high efficiency, easy usage, low maintenance requirements, and carbon neutrality. The electrolyzer uses the excess electricity to separate water into oxygen (air), which is fed to the cathode, and hydrogen is fed to the positive electrode (anode) by feeding DC power through two electrodes.

$$Electricity + H_2O \rightarrow H_2 + \frac{1}{2}O_2 \tag{2}$$

The output power that the hydrogen tank receives from the electrolyzer can then be expressed as follows:

$$P_{out-H_{2(t)}} = P_{in-ele} * \eta_{ele} \tag{3}$$

where,$P_{out-H_{2(t)}}$ represent the output power of electrolyzer, P_{in-ele} represent the input power of electrolyzer and η_{ele} represent the efficiency of electrolyzer. Finally, the following equation can be used to calculate the fuel cell plant's total generated power:

$$P_{FC(t)} = P_{H_2-FC} * \eta_{FC} \tag{4}$$

Modelling of battery

A battery is utilized in this research to measure the power to load and store any excess power generated[37]. In this situation, it is crucial to take the state of storage (SOC) into account. In fact, there are two modes such as charging and discharging. The charging process is expressed as follows:

$$P_{ch}(t) = (P_{WT}(t) + P_{PV}(t)) - (P_1(t)/\mu_{inv}) \tag{5}$$

where $P_{PV}(t)$, $P_{WT}(t)$ and $P_1(t)$ represent the power produced by the PV system, wind turbine and load power respectively. Whereas, μ_{inv} represent the converter's efficiency. Additionally, since hourly iteration time is employed, $C_{ch}(t)$ could be used in place of $P_{ch}(t)$. The charging mode can be expressed as follows:

$$C_b(t) = C_b(t-1) + C_{ch}(t) \tag{6}$$

The Eq. (7) is subject to the following requirement:

$$C_{ch}(t) \leq C_{b\ \max} - C_b(t) \tag{7}$$

where $C_b(t-1)$ represents the battery's condition at the previous moment and $C_{b\ \max}$ represents its maximum state. Otherwise, another expression will be taken into consideration in the event that an excessive load results in a wasted energy case:

$$\begin{cases} C_{dump}(t) = C_{ch}(t) - (C_{b\ \max} - C_b(t)) \\ C_{dump}(t) = 0 \end{cases} if \begin{cases} C_b(t) = C_{b\ \max} \\ else \end{cases} \tag{8}$$

where, $C_{dump}(t)$ presents the excess energy at time t. The discharging process is expressed as follows:

$$P_{dch}(t) = (P_1(t)/\mu_{inv}) - (P_{WT}(t) + P_{PV}(t)) \tag{9}$$

$P_{dch}(t)$ can also be substituted with $C_{dch}(t)$ because hourly iteration time is utilized. One way to express the discharging mode is as follows:

$$C_b(t) = C_b(t-1) - C_{dch}(t) \tag{10}$$

The state of charge for a time (t) is represented by $C_b(t)$, and this expression is subject to the following condition:

$$C_{dch}(t) \leq C_b(t-1) - C_{b\ \min} \tag{11}$$

where,$C_{b\ \min}$ represent the minimum state of the battery.

Modelling of EV

During motion, EVs must overcome a number of resistive forces, which must be taken into account when dynamically modelling the vehicle[34]. This model makes it possible to calculate the energy required for the electric drive forces and power as well as the theoretical electric vehicle load for each drive. Consequently, using EVs provides both power and energy, depending on the vehicle's speed in relation to the driving cycle. However, a number of metrics, such as fuel consumption and pollution levels, are used to evaluate a vehicle's performance. In EV modelling, a variety of roads, velocities, and forces are used. The load is determined by the sum of all forces, which is expressed as:

$$F_L = F_J + F_R + F_f + F_C \tag{12}$$

$$\begin{cases} F_J = 0.5.\phi.W.K_U.N_{EV}^2 \\ F_R = (L_{EV} + L_{ESS}).\left(K_0 + K_1 + L_{EV}^2\right) \\ F_f = (L_{EV} + L_{ESS}).\mathrm{Sin}(\beta).f \\ F_C = (L_{EV} + L_{ESS}).\left({}^{uN_{NU}}/_{dt}\right) \end{cases} \tag{13}$$

where L_{ESS} represent the mass of energy storage system, L_{EV} represent the mass of EV, the load force is represented by F_L, F_f represent the gravitational force, F_R represent the rolling resistance, F_C represent the acceleration force, ϕ represent the electric density, K represent the drag constant, W represent the area, N_{EV} represent the vehicle speed and f represent the gravitational constant.

Control strategy

Figure 2 shows the configuration of proposed energy management in EVs. The PV system, which acts as the primary source in DC MG, is connected to the DC bus through a BC. To maximize solar power extraction, an MPPT system based on the incremental conductance approach is employed. This comprises calculating the duty cycle, generating pulse width modulation (PWM), and accounting for the PV's voltage (V_{PV}) and current (I_{PV}). Consequently, control signals are produced for the BC. Because it effectively monitor peak power despite quickly fluctuating environmental circumstances, the incremental conductance technique has various advantages[22].A PI-based controller[29] controls the bidirectional converter as well as the BC[30] that joins the fuel cell and battery. By avoiding the use of error derivatives, the PI control technique enhances system stability when data noise is present. This is explained by the fact that the input from the PI is less vulnerable to abrupt and substantial state changes of the model in the absence of derivative intervention. A balanced mode is maintained by synchronizing the operation of many sources, particularly during fluctuations in solar irradiation.

Using a battery, the fuel cell and the load are connected. The PWM generator supplies the switching signals for the fuel cell's DC–DC BC, while the PI controller establishes the duty ratio. The PI controller's feedback loop computes the error signal using both the load voltage differential and the voltage reference. The DC-DC bidirectional converters are important for connecting the battery source to the MG as they charge and discharge electricity while in use. In order to provide a switching pulse for the bidirectional converter, the PI controller creates an error signal by comparing several factors, such as the current values from the PV BC, FC BC, and load. The DC-bus voltage and converter performance are directly impacted by the rapid and irregular changes in power demand caused by the EV charging and discharging profile. The control approach continuously monitors EV loading circumstances and modifies the converter duty cycle to handle these variations. In the case of unexpected EV charging surges or discharging events, this ensures constant power supply. Under dynamic EV behavior, the optimized-PI-fuzzy based hybrid energy model improves overall voltage stability.

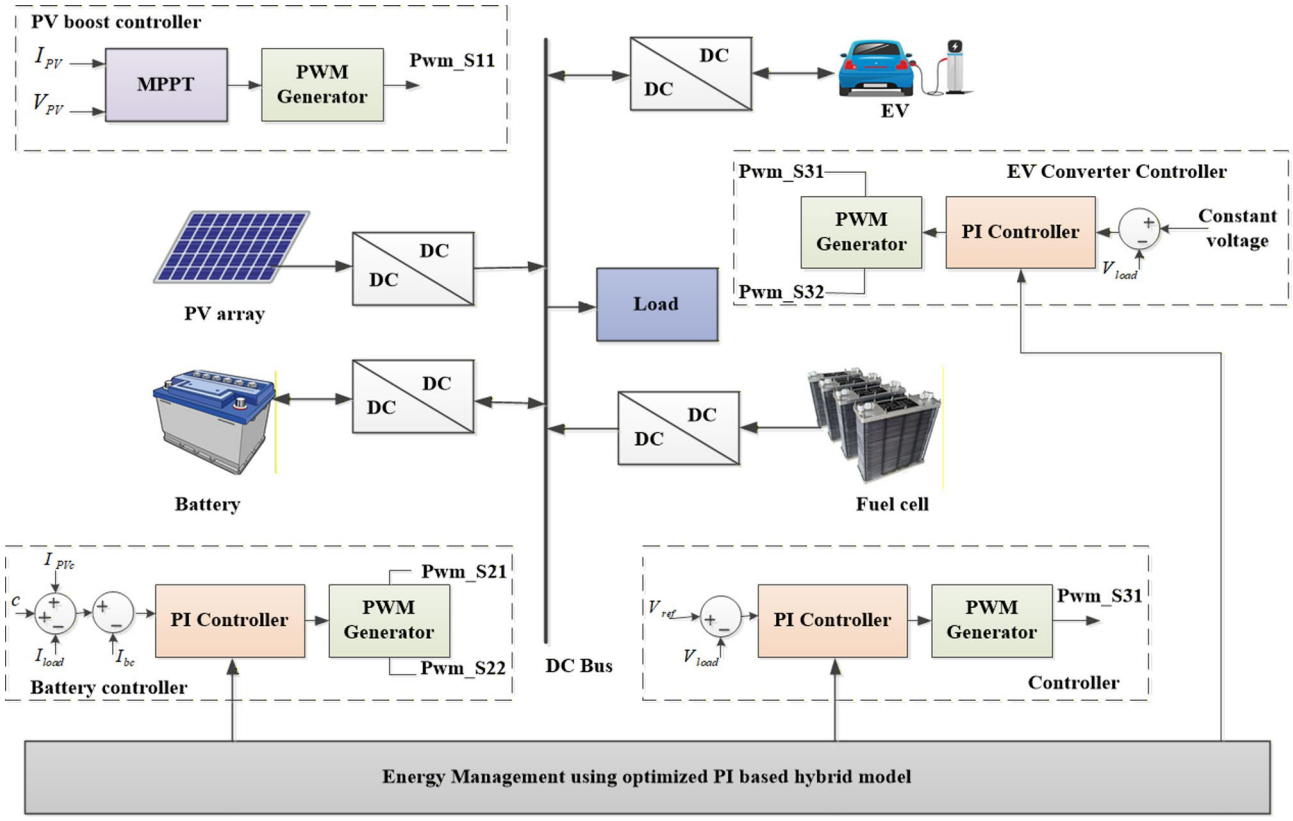

Fig. 2. Configuration of proposed energy management in EVs.

For the PI controller, the DMRPO is used to adjust the integral (k_i) and proportional (k_p) gain levels. The control logic determines the direction of energy flow among various parameters while accounting for operating conditions. The Hybrid DMRPO algorithm's optimal solutions for the PI controller and the solution from the Fuzzy controller are computed and used to produce the control signal for converters. To achieve the best power management, the controller combines the advantages of fuzzy controllers with DMRPO -based PI controllers. The control system is schematically depicted in Fig. 3.

A fuzzy logic controller's rule basis[31] is designed to produce a consistent and timely state response for slight changes in its inputs; the controller's output varies very little, ensuring precise control. The basic components of a fuzzy logic controller are fuzzification, defuzzification, fuzzy interface, and rule foundation. The choice of control variables is carefully studied when constructing the fuzzy control. Here, fuzzy logic control uses the error and its derivative as inputs. When creating input and output rules, they rely on membership functions rather than rigorous procedural needs. Figure 4 shows the fuzzy logic controller.

In the suggested EVCS model, the controller performance is improved by combining the control signal from the fuzzy control with the DMRPO Optimized PI controller.

Dwarf Mongoose-based Red Panda Optimization algorithm

This section involves tuning controller parameters such as K_p and K_i using the proposed DMRPO model. The suggested DMRPO is a hybrid metaheuristic that merges the exploratory advantages of Dwarf Mongoose Optimization (DMO) with the exploitation and defense mechanisms of the Red panda optimization (RPO). DMRPO looks for the best proportional and integral gains (K_p and K_i) of a PI controller that reduce a closed-loop performance index for the DC microgrid converters. A PI parameter vector is encoded by each candidate solution (red panda/mongoose). The mathematical model of this improved strategy are explained below:

Dwarf Mongoose Optimization (DMO) Three social groups are used by the dwarf mongoose (DM) population in the DMOA: scouts, babysitters, and the alpha group. Together, the family forages, with the alpha female starting the process and deciding on the sleeping mounds, distance travelled, and foraging route. Babysitters are provided by a portion of the DM population, which is typically a mix of male and female kinds. Until the remainder of the group shows up in the afternoon, they remain behind with the kids. First, the babysitters are switched so they can start foraging with the group (exploitation phase). Instead of building a nest to lodge the young, the DM group constantly shifts the sleeping mound in search of a new location for foraging. In an area big enough to fit everyone in the party, the DMs have developed a seminomadic way of living (exploration phase). The mathematical model of DMO is quoted as follows:

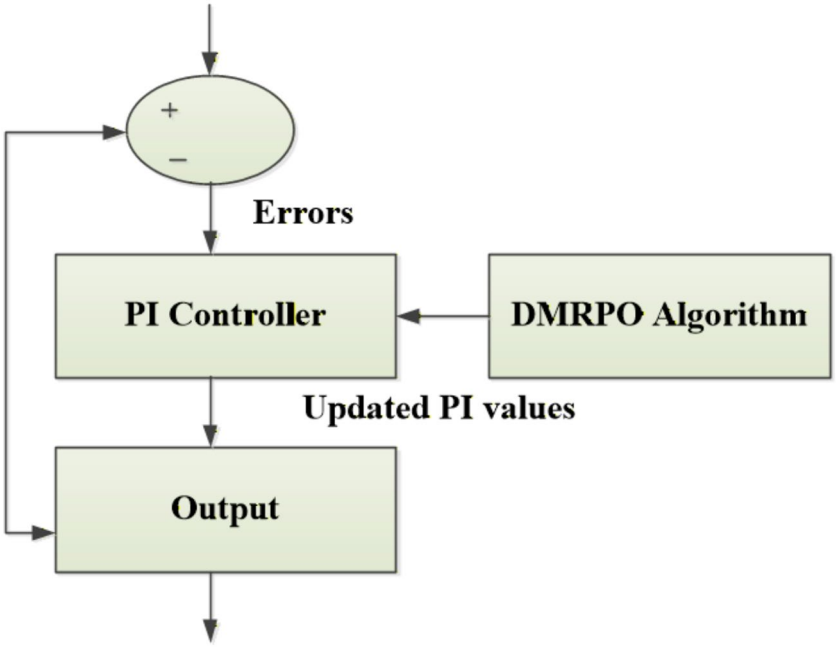

Fig. 3. DMRPO-PI control mechanism.

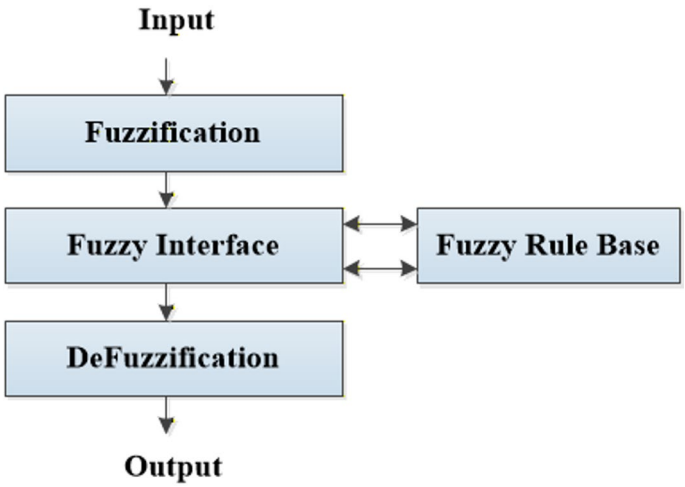

Fig. 4. Fuzzy Logic Controller Operation.

The initial DM populations of individuals potential solutions in the DMOA are produced at random in the manner described below:

$$P_{i,p}(0) = P_{\min,p}. + rand(0,1) \cdot \left(P_{\max,p} - P_{\min,p}\right), i = 1 : N_{PM}, p = 1 : Pim \tag{14}$$

where $P_{\min,p}$ and $P_{\max,p}$ indicate the minimum and maximum boundaries of each control variable (p);$P_{i,p}$ indicates the location as a seeking individual;Pim describes the number of choice variables associated with the optimization task.

Fitness function: After the population has been established, each solution's fitness is determined. The objective of optimization is to minimizing charging cost. The fitness function is expressed as

$$Fitness(F_i) = MIN(\cos t) \tag{15}$$

Alpha group: After the population is initialized, each solution's fitness is determined. The alpha female (α) is selected based on the probability value of each group's fitness, which is calculated by Eq. (16).

$$\alpha = \frac{F_i}{\sum_{i=1}^{N_{PM}} F_i} \tag{16}$$

The number of DMs in the alpha group is correlated with the difference between the number of babysitters and the overall group number (N_{PM}). B represents the number of babysitters. $Peep$ is the vocalization of the alpha female that keeps the DM family on course. To determine a possible food position, the DMOA uses the formula given in Eq. (17).

$$P_{k,p}(j+1) = P_{k,p}(j) + rand(0,1) \times peep, k = 1 : N_{PM} - B, p = 1 : Pim \tag{17}$$

where j indicate the existing iteration. Following each iteration, the sleeping mound can be expressed as follows:

$$SM_i = \frac{F_{i+1} - F_i}{Max\left[|F_{i+1} - F_i|\right]} \; i = 1 : N_{PM} - B \tag{18}$$

where i refers to each DM in the scout group which are the difference between the whole group number (N_{PM}) and the number of babysitters (Bst). The mean value χ of the sleeping mound is expressed in Eq. (19).

$$\chi = \frac{\sum_{i=1}^{N_{PM}} SM_i}{N_{PM}} \tag{19}$$

Scout group: When the babysitting exchange condition is met, the DMOA approach moves on to the scouting step, when a subsequent food source or sleeping mound will be identified. In order to ensure exploration, scouting takes place in conjunction with foraging in DMOA. The scouts look find a different sleeping mound. Based on the mongooses overall performance, the ensuing action is portrayed as a successful or failing evaluation of creating a new mound. Equation (20) can model the scout mongoose.

$$P_{k,p}(j+1) = \begin{cases} P_{k,p}(j) - CF \times rand(0,1) \times [P_{k,p}(j) - M], & if\ \chi_{i+1} > \chi_i \\ P_{k,p}(j) + CF \times rand(0,1) \times [P_{k,p}(j) - M], & otherwise \end{cases} \tag{20}$$

where $rand$ denotes the random number within the range of 0 to 1, M denotes a vector that determines the mongoose's migration to the next sleeping mound, as shown in Eq. (22), and CF decreases linearly as iterations go on, as shown in Eq. (21). The parameter that controls the collective-volitive motion of the mongoose group is denoted by the CF parameter.

$$CF = \left(1 - \frac{j}{Max\_t}\right)^{\left(2 \times \frac{j}{Max\_t}\right)} \tag{21}$$

$$M = \sum_{i=1}^{N_{PM}} \frac{P_i \times SM_i}{P_i} \tag{22}$$

where Max_t denotes the maximum number of iterations. Smaller group members, known as babysitters, are typically in charge of the young ones. In order for the mother, the alpha female, to lead the other members of the squad on the daily hunting, they are continuously replaced.

Red Panda Optimization (RPO) The red panda is a small, native mammal found in the eastern Himalayas and southern China. The red panda's foraging technique, which relies on its acute senses of smell, hearing, and sight as well as its exceptional ability to climb trees, is one of its most remarkable natural activities. The mathematical modeling of these red panda natural behaviors is provided below.

The population matrix of RPO algorithm is formulated as:

$$Y = \begin{bmatrix} Y_1 \\ \vdots \\ Y_i \\ \cdot \\ Y_N \end{bmatrix}_{N \times m} \tag{23}$$

where Y represent the population matrix of red pandas' locations, Y_i represent the i^{th} red panda, N represent the number of red pandas and m represent the number of problem variables.

Foraging Strategy (Exploration): Red pandas' movement to forage in the wild is used to mimic their position in the first stage of RPO. Red pandas use their keen senses of smell, hearing, and eyesight to locate food sources and move in that direction. Using Eq. (24), a new position is initially determined for each red panda based on movement towards the location of the food supply (the best candidate solution) in order to represent the behavior of red pandas while foraging. The red panda's position is then changed to the location determined during the exploration phase using Eq. (25) if the objective function's value improves at the new location.

$$Y_i^{D1} : Y_{i,j}^{D1} = y_{i,j} + r.(sfs_{i,j} - I.y_{i,j}) \tag{24}$$

$$Y_i = \begin{cases} Y_i^{D1}, & F_i^{D1} < F_i \\ Y_i, & otherwise \end{cases} \tag{25}$$

Where Y_i^{D1} represents the i^{th} red panda's new position based on the first phase of RPO, $Y_{i,j}^{D1}$ represents its j^{th} dimension, Y_i^{D1} represents its objective function value, sfs_i is the i^{th} red panda's chosen food source, $sfs_{i,j}$ denotes its j^{th} dimension, r is a random number in the interval [0, 1}, and I is a random number chosen at random from the set {1, 2}.

Proficiency in climbing and resting on trees (exploitation): Red pandas' ability to climb trees and rest on them is used to depict their position in the second phase of the RPO. Red pandas rest on trees for the majority of the day. This animal climbs the surrounding trees after foraging on the ground. Red pandas' positions shift slightly as they approach and ascend the tree, which improves the suggested RPO algorithm's capacity for local search and exploitation in promising regions. First, a new position is determined for each red panda utilizing Eq. (25) to mathematically simulate their natural behavior when climbing trees. The matching red panda's original position is then replaced with this new position using Eq. (26) if the objective function's value is improved.

$$y_{i,j}^{D2} = y_{i,j} + \frac{LB_j + r \cdot (UB_j - LB_J)}{t} \tag{26}$$

$$Y_i = \begin{cases} Y_i^{D2}, F_i^{D2} \leq F_i \\ Y_i, Otherwise \end{cases} \tag{27}$$

where $y_{i,j}^{D2}$ represents the i^{th} red panda's new position based on the second phase of RPO, $y_{i,j}^{D2}$ represents its j^{th} dimension, F_i^{D2} represents its objective function value, r represents a random number in the interval [0, 1], t represents the algorithm's iteration counter. Figure 5 shows the flowchart of proposed DMRPO algorithm.

The original approaches, DMO[32] and RPO[33], include issues such early convergence, asymmetries in the search process, and poor convergence capacity. These issues are intended to be addressed by the hybrid methodology. The major updating technique of DMO is applied in a suggested manner to increase the search functionality of RPO. The proposed method's pseudo-code is described in Algorithm 1, which mainly uses two important

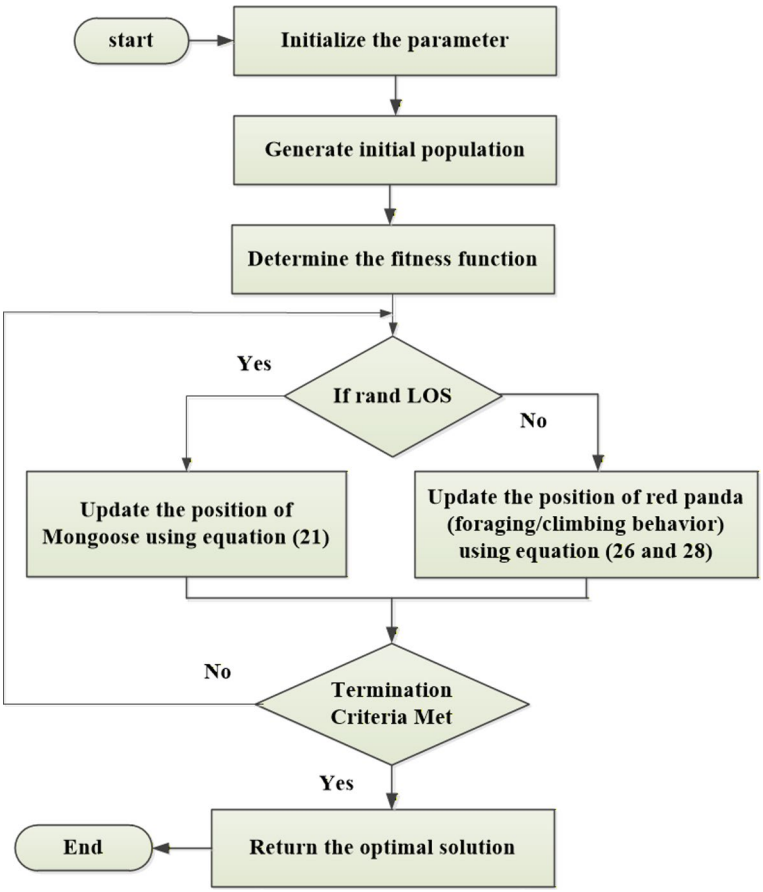

Fig. 5. Flowchart of proposed DMRPO algorithm.

Input: Define the algorithm's parameters and solutions.

Initialize the solutions and parameters.

While $(Iter < Max\_I)$ do

Compute the fitness of each solution

For $i = 1\ to\ N$

If $(Rand < 0.5)$

{

\\Update solution by DMO

{

Select the alpha mongoose using Equation (16)

Generate candidate food location using Equation (17)

Compute sleeping mound by Equation (18)

Compute mean sleeping mound using Equation (20)

Update the scout mongoose position using Equation (21)

}

Else

\\ Update the solutions by RPO

{

Compute new position using foraging behavior using Equation (25)

Update position using Equation (26) if fitness improves

Compute new position using climbing behavior using Equation (27)

Update position using Equation (28) if fitness improves

}

End if

End For

$t = t + 1$

End while

Output: Return the optimal solution

Algorithm 1: Pseudo-code of DMRPO algorithm.

search operators. If the random value $(Rand)$ is less than 0.5, one of the RPO or DMO operators is used. The presence of low diversity is usually noticed when one of the optimization strategies updates the candidate solutions, influencing the performance of the search operators. Furthermore, a lack of diversity in the solutions utilized leads to an imbalance in the search process, with operators focused either on local or global search, hurting one side of the updating processes. As a result, the alternating use of search approaches in the suggested strategy improves search performance and ability, leading to more robust solutions. This modification is done to

prevent imbalances and early convergence among the search operators. Algorithm 1 offers the pseudo-code for the proposed hybrid strategy and Fig. 6 depicts the flowchart of the methodology.

Results and discussions

An MG model with batteries, fuel cells, and solar panels uses an optimized PI-based hybrid model to manage energy. The DC MG module is designed using MATLAB/Simulink, and the power converters and energy sources are built within the Simulink environment using Simscape. While Simscape serves as the actual modeling component, it also provides a graphical programming structure for creating, testing, and evaluating model behavior. The proposed DMRPO was used to optimize the K_p K_i and PI controller parameters, and the obtained solutions were integrated with fuzzy logic control. Variations in Battery State of Charge (SoC) and a range of solar irradiation levels were used to control the MG in various operating modes, guaranteeing a steady power supply for EV charging on a DC MG. The results and evaluation of the presented model in different contexts are covered in this section. The elements of the developed DC MG model are shown in Table 2, and the control parameters and their operating ranges are shown in Table 3. Table 4 shows the Controller settings and algorithmic details.

Simulation settings

Time-step configuration: To accurately capture converter-level dynamics, a fixed-step solver with a sampling time of 1 s was used. Data were logged at intervals of one minute to ensure readability and clarity in the plots that were produced.

Number of runs: To include renewable and EV-arrival variability:

- Three RE-penetration scenarios were simulated (84%, 52.5%, 20.1%)
- 10 Monte-Carlo runs per scenario were performed

Figure 7 shows the optimized PI-based hybrid model.

The findings of the fuzzy controller, which show how input variables are described for optimal EV charging management, are displayed in Fig. 8. Three categories comprise the membership functions for EV power demand, as shown in Fig. 8 (a): Low 0–7 kW, Average 7–13 kW, and High 13–19 kW. Since an EV's power requirement depends on both battery capacity and state of charge, this represents the demand variability caused by these two elements. Due to their different battery capacity and states of charge (SOC), EVs have different power requirements at the charging station. The majority of EVs are often charged at night, and while vehicles with greater SOC need less time to fully charge, smaller vehicles like autorickshaws and cycles take 8 to 10 h. The production of electricity is shown in Fig. 8 (b). Based on RES availability, the fuzzy sets Insufficient 0–6 kW, Fair 6–13 kW, and Sufficient 13–19 kW show the range of renewable power availability from low to high. As shown in Fig. 8 (d), the charging time is divided into Peak Hours (0–6 h), when demand is at its peak and grid stress is at its maximum, and Off-Peak Hours (6–20 h), when demand is lower and charging is more favourable. Finally, Fig. 8 (c) depicts the existing tariff as Fixed for all hours 0–24, indicating that the cost of charging is constant throughout all time slots. The Mamdani-type fuzzy inference system with centroid-based defuzzification can ascertain the charging current and renewable utilization levels due to these membership functions, which are modelled using triangle, trapezoidal, and Gaussian functions. This ensures that EV charging adapts dynamically to variations in supply (0–19 kW), demand (0–19 kW), and charge duration (0–24 h) while maximizing the integration of renewable electricity and maintaining cost effectiveness. When PV and FC outputs were high, the controller automatically prioritized renewable energy, allowing the EMS to achieve a decrease in net tariffs with growing net power generation. The system relocated EV charging into low-cost renewable hours, decreased grid

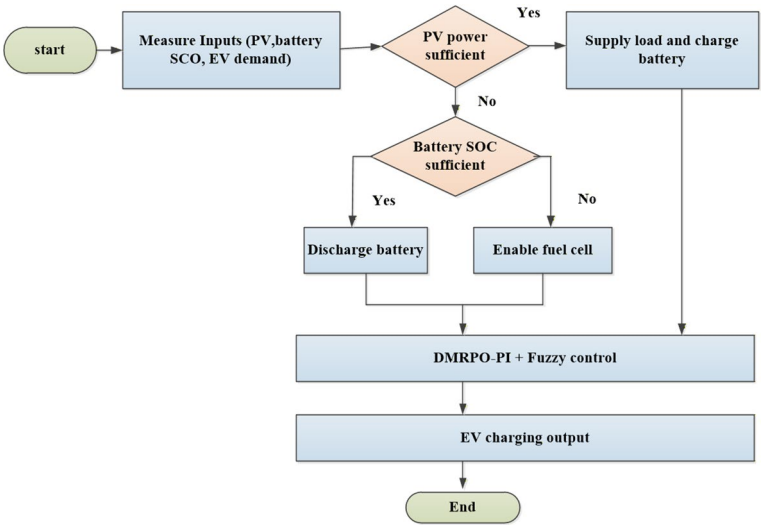

Fig. 6. Proposed methodology flowchart.

Component	Factors	Range
Li-ion Battery	Capacity	48Ah
	Fully charged voltage	290.9968 V
	Cut-off voltage	187.5 V
Solar PV	Irradiance	1000 W/m^2
	Short Circuit Current	8.67 A
	Parallel strings	8
	Temperature	25℃
	Maximum Power	300.366 W
	Open Circuit Voltage	45 V
	Series Connected Modules per string	5
Solar PV BC	Input Resistance Inductor	12 Ω
	Input Capacitor	0.48μF
	Input Inductance	1.2 mH
Fuel Cell	Total cells	65
	Nominal cell voltage	1.2101 V
	Normal Air Flow Rate	300 L/min
	Normal Composition(H_2, O_2, H_2O)	(99.95,21,1)
	Operating Temperature	65 Celsius
	Normal Stack Efficiency	55%
	Normal Supply Pressure[Fuel, Air]	(1.5 ,1)bar
	Fuel cell resistance	2.3677 ohms
Fuel Cell BC	Input Inductance	3.6mH
	Input Resistance	2.36Ω
	Input Capacitor	0.13μF
	Output Capacitor	0.16μF
Bidirectional converter	Inductance	1.4 mH
	Input Capacitor	1.16 μF

Table 2. Simulation parameters.

Subsystem	Parameter (symbol / unit)	Role in control	Operating range / limits
MPPT (IncCond)	Perturbation limit on VpvV_{pv} (%)	MPPT step bounding	± 2% of VpvV_{pv}
DC Bus	DC-link reference Vdc* (V)	Outer voltage loop set-point	400
DC Bus	Allowable band for Vdc (V)	Voltage regulation target	380–420 (± 5%)
Fuel Cell + DC/DC	FC power PfcP_{fc} (kW)	Dispatch limit	0–5
Fuel Cell + DC/DC	FC ramp-rate (W/s)	Dynamic constraint	≤ 100
Scenario knobs (for results)	EV charging demand (kW)	Load case definition	Low ≤ 8, Medium 8–14, High > 14
Scenario knobs (for results)	RE penetration (%)	Mix for GHG/Cost	20.1, 52.5, 84
Fuzzy controller	Input universes e, Δe (pu)	Rule-base inputs	[− 1,1][-1,1]
Fuzzy controller	Output universe u (pu)	Duty/command increment	[0,1][0,1]
Battery + Bi-DC/DC	State of charge SoC (%)	Energy mgmt. limit	20–90 (normal); 10–95 (hard)
Battery + Bi-DC/DC	Charge/discharge C-rate (C)	Current limiting	0.5–1C cont., 1–2C peak (≤ 10 s)
Battery + Bi-DC/DC	Duty cycle DbiD_{bi} (pu)	Buck/boost actuator	0.05–0.95
Controllers (PI tuned by DMRPO)	K_p, K_i – PV boost	Inner current/voltage loops	Kp ∈ [0,5], Ki ∈ [0,500]
Controllers (PI tuned by DMRPO)	Kp,Ki– DC bus	Bus voltage loop	Kp ∈ [0,10], Ki ∈ [0,1000]
Controllers (PI tuned by DMRPO)	Kp,Ki – Bi-DC/DC	Battery current loop	Kp ∈ [0,5], Ki ∈ [0,500]
PV + Boost	Irradiance GG (W/m^2)	Scenario input for MPPT	200–1000
PV + Boost	Cell temperature TT (°C)	Scenario input for MPPT	15–55
PV + Boost	PV voltage VpvV_{pv} (V)	MPPT measured variable	0.6–0.95 of VocV_{oc}
PV + Boost	Duty cycle DpvD_{pv} (pu)	MPPT/boost actuator	0.05–0.90
PV + Boost	PWM frequency fpwmf_{pwm} (kHz)	Converter switching	10–25

Table 3. Control parameters and its operating ranges.

Parameter (symbol)	Description (Tamil)	Value (example)	Unit
K_p	Proportional gain of PI	0.8	—
K_i	Integral gain of PI	50	s^{-1}
Sampling time (T_s)	Controller sampling period	0.001	S
DMRPO population	Optimization population size	30	individuals
DMRPO iterations	Max iterations	100	iterations
Fitness tolerance	Convergence threshold	1e-6	—
$(V_{dc,ref})$	DC bus reference voltage	400	V
Ramp rate	Charging ramp limit	0.5	kW/s
Simulation duration	Total sim time	3600	s (1 h)

Table 4. Controller settings and algorithmic details.

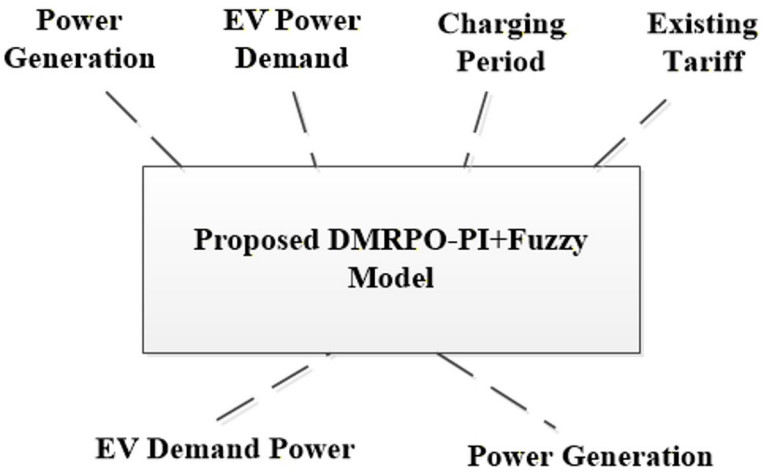

Fig. 7. DMRPO-PI-based fuzzy model.

import as RES availability increased and used optimal PI-based evaluations to minimize consumer charging costs. Higher on-site generating therefore directly led to lower tariffs for the customer.

The results of the proposed approach are displayed in Fig. 9. Figure 9 (a) shows the variation in charging costs with respect to EV power usage. At low demand levels of 1–5 kW, the cost of charging is constant at roughly 2–2.2 USD/kWh. When demand exceeds 6 kW, costs start to increase significantly. They peak at roughly 5.5 USD/kWh when demand is between 9 and 10 kW, after which they level out. This pattern highlights the charging expenses are more expensive during periods of high demand and less expensive during periods of low or off-peak demand. This dynamic method enhances grid load balancing by encouraging electric vehicle owners to choose off-peak charging periods. Figure 9 (b) shows the relationship between charging costs and power generation, with charging costs remaining largely constant at 5.8–6 USD/kWh up to an 11 kW generation. After that, as power generation increases, the cost of charging begins to decline dramatically and virtually vanishes when generation reaches 16–18 kW. This implies that EV users charge more affordably when renewable energy is more accessible, which promotes charging during periods when solar resource contribution is high. Conversely, when generation is limited due to an increased reliance on conventional grid electricity, charging costs rise. Figure 9 (c) shows the use of renewable energy as a function of power generation. Initially, renewable usage is quite low up to about 5–6 kW. It then starts to gradually rise. Between 10 and 15 kW, utilization rises sharply from around 7 to 16 kW before stabilizing at about 17 to 18 kW when generation is at its peak. This clearly shows the charging infrastructure's integration of renewable energy sources supports sustainability targets by lowering charging costs and increasing available power. All things considered, dynamic tariff adjustment is demonstrated by the proposed PI-based hybrid EVCS model. Current EVCS systems maintain customer charging costs between 1.600 and 1.8666 USD/kWh, with a regulated base rate of 0.0817 USD/kWh. The proposed strategy accounts for a few factors, such as EV demand, charging time, and the availability of renewable energy. This ensures that EV users pay less when renewable resources are plentiful and supports grid stability by restricting excessive use during demand peaks.

Figure 10 shows the time-varying charging cost (USD/kWh) for different EMS methods throughout a 24-h period. In order to ensure a fair comparison across all demand levels and charging intervals, all cost values are normalized using:

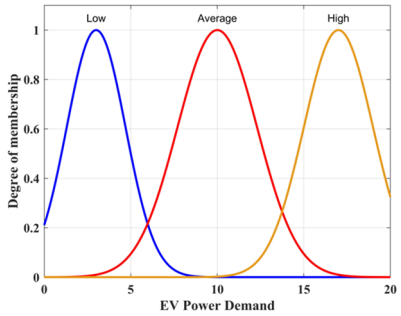

(a)

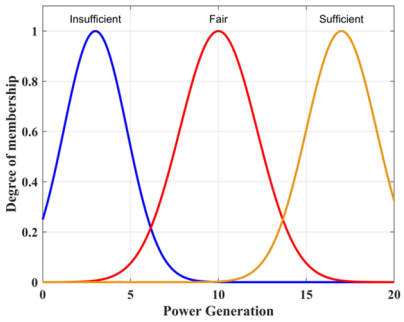

(b)

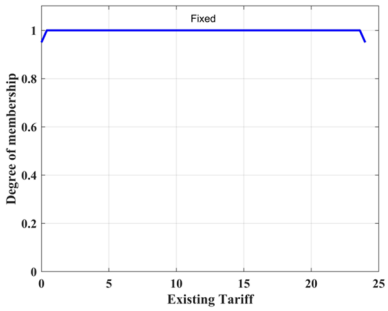

(c)

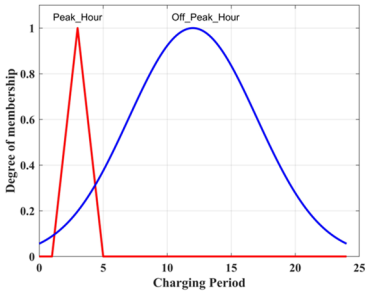

(d)

Fig. 8. Fuzzy controller outcomes (a) power demand of EV, (b) power generation, (c) Existing tariff (d) Charging period.

$$\text{Charging Costs (USD/kWh)} = \frac{Total\ charging\ \ cost\,(\text{USD})}{Energy\ delivered\ (\text{kWh})} \tag{28}$$

The CC varies throughout the day, with the biggest charges being during peak hours (6:00 PM to 10:00 PM). The ANN-based EMS ranged from 0.095 to 0.097 USD/kWh at peak hours, but the fuzzy-SSA technique records charging rates of 0.1054 USD/kWh at 6:00 PM, 0.1024 USD/kWh at 8:00 PM, and 0.1094 USD/kWh at 10:00

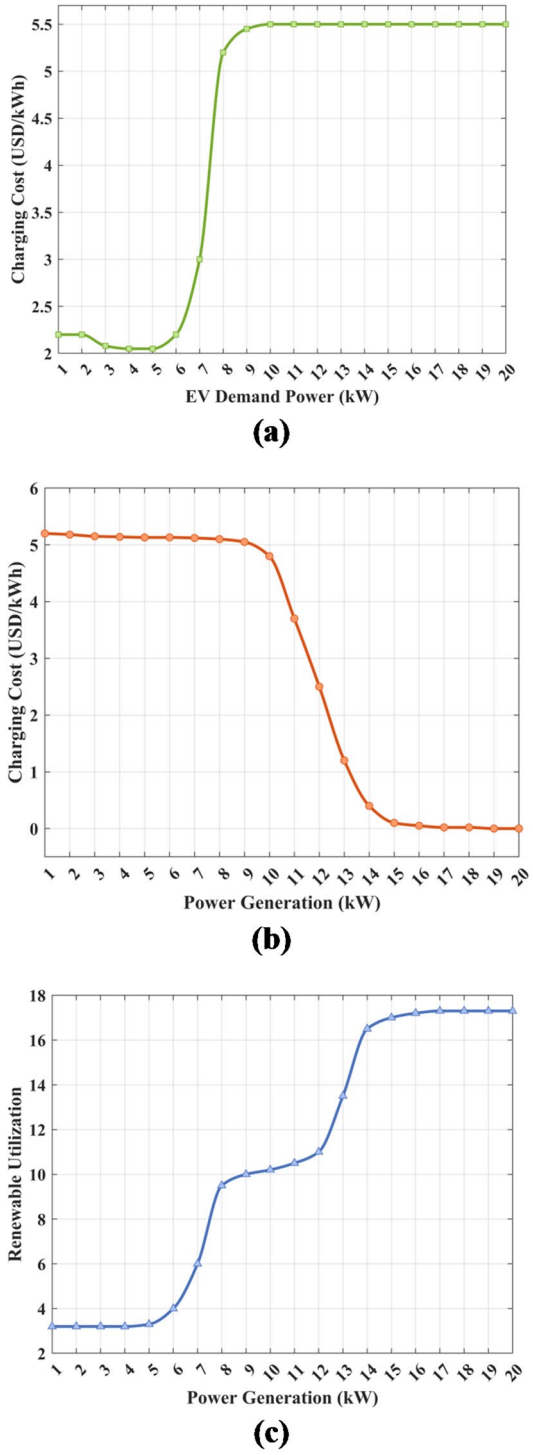

Fig. 9. Outcomes of proposed optimized PI-based hybrid model (a) EV power demand vs charge cost, (b) Power production vs charge cost, and (c) power generation vs RE usage.

PM. The proposed approach performs better by maintaining a much lower peak-hour CC of 0.06–0.061 USD/kWh. As electricity prices decline during off-peak hours, the CC for all algorithms lowers after 10:00 PM. In comparison to fuzzy-SSA (0.0274–0.0434 USD/kWh) and DNN-LSC (0.021–0.03 USD/kWh), the proposed method consistently produces the lowest values throughout the day, reaching a minimum CC of 0.009–0.015 USD/kWh between 10:00 AM and 2:00 PM. This proves that the proposed PI-based hybrid method reduces charging costs more successfully than traditional methods. When compared to peak-hour flat-rate tariffs utilized in many EVCS settings, the proposed method's lowest observed CC is 0.009 USD/kWh.

Figure 11 shows an analysis of CCs under various RE penetration scenarios compared to present ones. Encouraging EV users to recharge their batteries during off-peak hours could help minimize demand during

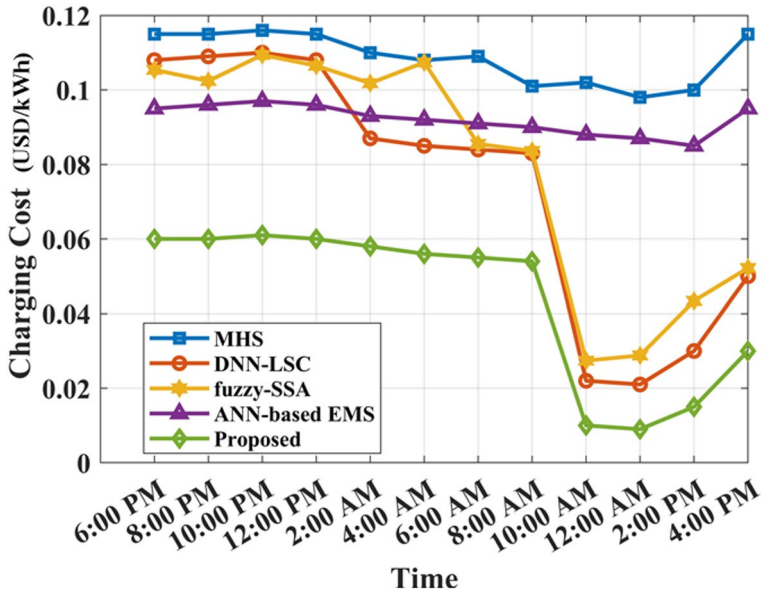

Fig. 10. Comparing time-varying charging costs using various EMS techniques.

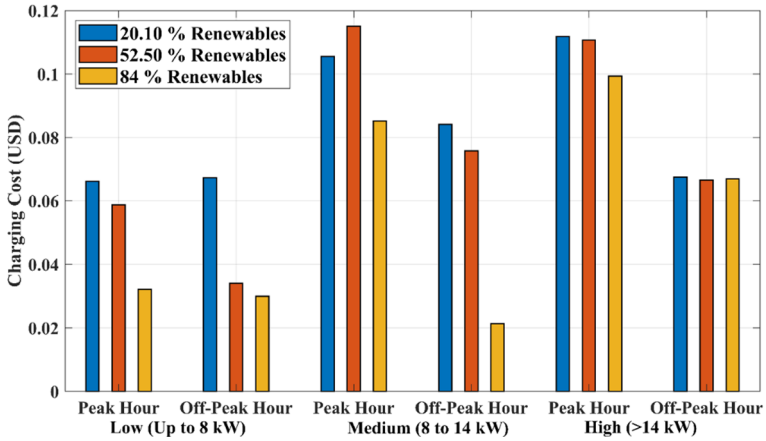

Fig. 11. CC evaluation of the proposed algorithm.

peak hours. Solar energy during the day not only maximizes the use of RES but also minimizes the quantity of additional batteries required for the EVCS. The proposed approach encourages the incorporation of hybrid RES in EV CSs, strengthening the distribution network, by reducing EV load demand during peak hours. By encouraging EV owners to recharge their batteries during off-peak hours, when renewable utilization is at its highest, the proposed algorithm improves the overall energy management strategy while lowering prices for consumers. Additionally, this energy management approach significantly lowers greenhouse gas emissions as compared to conventional utility grid-based EVCS, supporting environmental sustainability.

The greenhouse gas discharges from the proposed EVCS and a typical grid-connected EVCS are contrasted in Fig. 12. The graph shows that as more RE is used, there is less needed to draw energy from the utility system to satisfy the increased demand for electricity than what is produced, which lowers indirect greenhouse gas emissions than traditional approaches, like MHS, DNN-LSC Fuzzy-SSA, and ANN-based EMS. It is possible to reduce greenhouse gas emissions to a maximum of 54.8% by utilizing a combination of 84% RE and 16% fossil fuel. The chart shows that a drop in GHG emissions from the EVCS is correlated with an increase in the use of RE.

Standard power emission factors were used to compute operational GHG emissions to assure transparency of the reported 54.8% reduction. Fossil fuel-based electricity was subject to a grid emission factor of 0.82 kg CO2/kWh, and renewable energy sources (PV and FC operation) were determined to have zero emissions during operation. The emissions that were prevented were observed by:

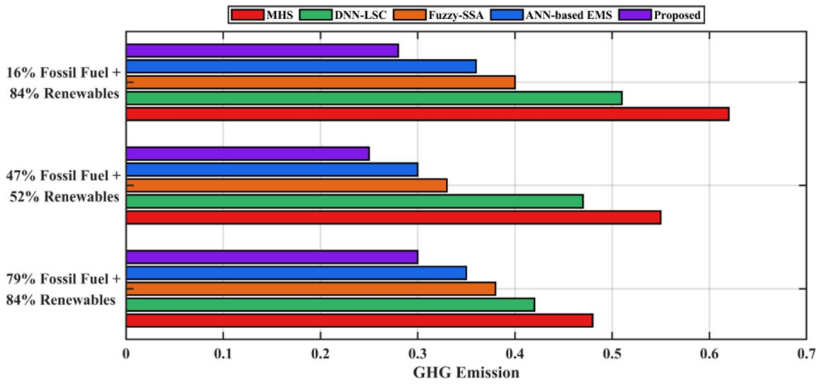

Fig. 12. GHG emission comparison.

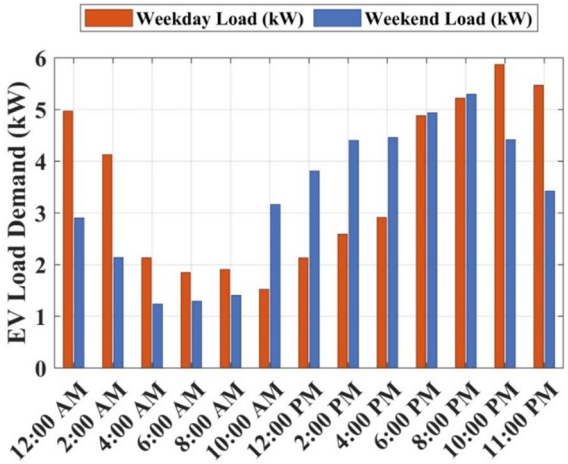

Fig. 13. Load profile of EV.

$$GHG\ reduction\,(\%) = \frac{E_{grid,existing} - E_{grid,proposed}}{E_{grid,existing}} \times 100 \tag{29}$$

where, $E_{grid,existing}$ is the amount of utility grid electricity required by existing EVCS, and $E_{grid,proposed}$ is the reduced grid energy demand achieved by the optimized PI based hybrid model EMS.

As shown in Fig. 13, the proposed optimization method is implemented on weekdays and weekends to evaluate its performance. On weekdays, EV drivers are more likely to arrive to the EVCS in the evening and remain till the next day. On the other hand, on weekends, EV drivers typically begin charging their vehicles at 10 AM and end it at midnight. Weekends have a lower charge fee since most charging occurs during off-peak hours, when solar energy is available. However, the majority of EVs arrive during peak hours on weekdays, when renewable power is scarcer and charging rates are higher. The simulation's findings indicate that the average cost of charging is 0.088 USD/kWh on weekends and 0.086 USD/kWh during the week. The new EVCS significantly reduces charging costs by 45.26% during the week and 56.11% during the weekend when compared to the average cost. The distribution network is significantly impacted by EV charging, particularly during peak load times when it increases power loss and voltage fluctuations. However, both consumers and the power infrastructure gain from charging during off-peak hours. Peak hours are from 5 to 11 PM, while off-peak hours are from 11 to 5 PM. Due to lower power consumption, the charge rate is lower during off-top hours than it is during top hours.

System stability is impacted by rapid EV charging and discharging events, which cause variations in DC-bus voltage and power balance. The proposed controller maintains voltage within bounds and reacts swiftly to these fluctuations. The controller ensures steady operation under various charging patterns and minimizes transients during sudden shifts in EV load.

The Table 5 presents the time-of-use pricing structure applied in this study for all charging-cost evaluations. A flat-rate value of 0.120 USD/kWh is defined as the single consistent baseline against which all reductions are measured.

The relationship between charging cost and solar irradiation throughout the day is depicted in Fig. 14. The charging cost is still high at 0.058–0.060 USD/kWh under low irradiance (200–300 W/m^2 between 6 PM and 8 AM). Between 11 AM and 12 PM, the cost decreases dramatically to 0.007–0.010 USD/kWh as irradiance

Time	Tariff Type	Cost (USD/kWh)
Peak	Peak	0.120
Off-Peak	Off-Peak	0.034
Weekend	Weekend	0.088
Weekday	Weekday	0.086

Table 5. Time-of-use tariff structure used for EVCS cost evaluation.

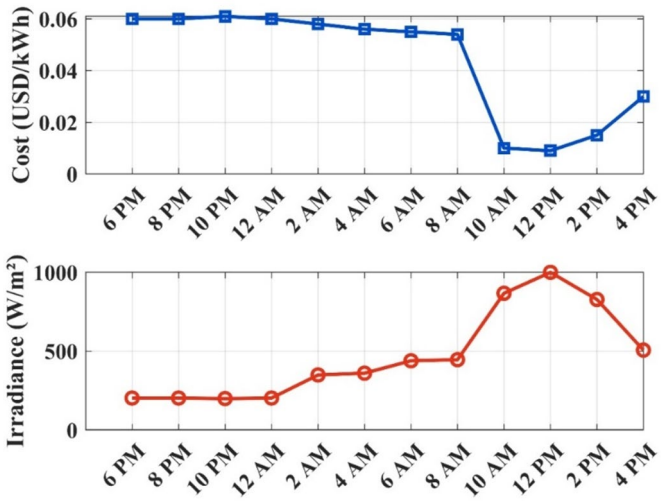

Fig. 14. Variation of Charging Cost and Solar Irradiance over a 24-Hour Period.

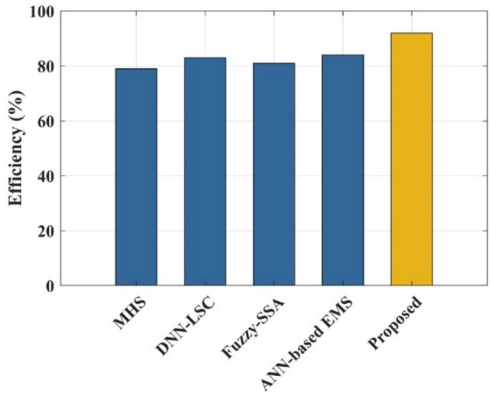

Fig. 15. Comparison of efficiency.

rises to 900–1000 W/m^2. The cost increases once more in the afternoon when irradiance decreases, indicating efficient use of renewable resources and steady EMS response.

Figure 15 compares the effectiveness of several EMS methods. While DNN-LSC[25] and Fuzzy-SSA[22] demonstrate marginal increases at 82% and 80%, respectively, the MHS[23] approach reaches about 78%. At 84%, the performance of the ANN-based EMS[26] is slightly higher. With an efficiency of almost 92%, the proposed optimized PI-based hybrid model performs better than all other techniques, indicating a significant advancement over current methods. This validates the better control stability and energy efficiency attained by the proposed approach.

The proposed DMRPO technique, as shown in Fig. 16, achieves the lowest and fastest convergence, drastically lowering the goal value from 0.25 to about 0.015 in the first ten rounds. By comparison, Whale Optimization Algorithm (WOA) drops from 0.24 to about 0.028, Particle Swarm Optimization (PSO) drops from 0.23 to almost 0.03, while Grey Wolf Optimizer (GWO) stays at 0.25 for several rounds until settling at almost 0.035. Among all approaches, DMRPO not only converges earlier but also achieves the lowest final value. These findings

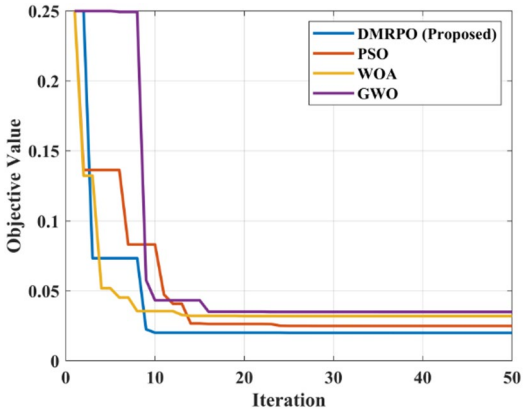

Fig. 16. Convergence analysis.

Case (RE % / Fossil %)	MHS	DNN_LSC	Fuzzy_SSA	ANN_based_EMS	Proposed
Case-A: 84% RE / 16% fossil	0.5	0.44	0.39	0.36	0.31
Case-B: 52.5% RE / 47.5% fossil	0.57	0.49	0.35	0.32	0.27
Case-C: 20.1% RE / 79.9% fossil	0.64	0.53	0.42	0.37	0.29

Table 6. GHG emissions (normalized units) across methods and cases.

Comparator / Case	Case-A	Case-B	Case-C
reduction in GHG vs EVCS	76.40%	68.15%	56.20%
reduction in GHG vs DMO + Fuzzy	63.85%	61.30%	50.75%
reduction in GHG vs RPO + Fuzzy	39.20%	33.90%	17.45%

Table 7. Relative improvement of the proposed method.

verify that, in comparison to other methods, DMRPO offers better optimization accuracy, faster convergence, and more consistent performance for controller tuning.

The GHG emissions (normalized units) for each technique and scenario are displayed in Table 6. With values of 0.31 in Case A, 0.27 in Case B, and 0.29 in Case C, the proposed optimized PI-based hybrid approach outperforms the other approaches and produces the lowest emissions in every cases. The relative improvement of the proposed approach (GHG reduction compared to the comparator, case-wise) is displayed in Table 7. By reducing GHG emissions by 76.40% when compared to EVCS, 63.85% when compared to DMO + Fuzzy, and 39.20% when compared to RPO + Fuzzy, the suggested method achieves the greatest decrease. These results show that the proposed approach consistently outperforms the benchmark methods, with the biggest effect being shown when renewable energy sources dominated.

Conclusion

For a DC microgrid-based electric vehicle charging station, this research presented an adaptive intelligent energy management system that combines battery storage, fuel cells, and photovoltaic generation. To improve power coordination and sustain stable converter performance under varying renewable energy availability and EV charging demand, a hybrid controller that combines fuzzy logic with DMRPO-optimized PI tuning was developed. By offering quicker convergence, enhanced stability, and reliable decision-making, the proposed optimized PI-based hybrid method effectively addressed significant shortcomings in current EMS systems. The optimized hybrid EMS significantly reduces operating costs, increases the use of renewable energy, and improves microgrid reliability, according to simulation results. During high-irradiance periods, charging prices were decreased to 0.009–0.015 USD/kWh, while average workday and weekend charges were lowered to 0.086 USD/kWh and 0.088 USD/kWh, respectively reductions of 45.26% and 56.11% when compared to traditional systems. Furthermore, a maximum decrease of 54.8% in greenhouse gas emissions was attained by the proposed approach, which was verified using corrected grid-energy calculations and standard emission factors. Even during fast EV charging and discharging events, voltage regulation and power balance were effectively maintained, demonstrating the controller's resilience in dynamic microgrid situations. Future research should

examine the implications of rapid battery charging and discharging as well as the fast-reaction properties of the hybrid algorithm for possible implementation in AC and hybrid microgrids.

Data availability

The datasets used and/or analyzed during the current study are available from the first author on reasonable request.

Received: 9 October 2025; Accepted: 16 February 2026
Published online: 24 February 2026

References

1. Gulraiz, A. et al. Leveraging dense layer hybrid graph neural networks for managing overvoltage in PV-dominated distribution systems. *Results Eng.* **27**, 106169 (2025).
2. Huy, T. H., Dinh, H. T., Vo, D. N. & Kim, D. Real-time energy scheduling for home energy management systems with an energy storage system and electric vehicle based on a supervised-learning-based strategy. *Energy. Conv. Manag.* **292**, 117340 (2023).
3. Ali, M., Vasquez, J. C., Guerrero, J. M., Guan, Y. & Lashab, A. February. Resilience assessment of mobile microgrid scenario for supporting critical infrastructure post-disaster. In *IET Conference Proceedings CP917, vol. 2025* 358–363 (The Institution of Engineering and Technology, 2025).
4. Andersen, P. H., Ali, M., Anvari-Moghaddam, A., Nielsen, R. P. & Simonsen, M. E. Re-purposing wind turbine blades: matching strategies and innovation governance forms. In *Proceedings of the 6th Product Lifetimes and the Environment Conference (PLATE2025)* (2025).
5. Ali, M. et al. A comparison of grid-connected local hospital loads with typical backup systems and renewable energy system based ad hoc microgrids for enhancing the resilience of the system. *Energies* **16** (4), 1918 (2023).
6. Barker, T., Ghosh, A., Sain, C., Ahmad, F. & Al-Fagih, L. Efficient ANFIS-driven power extraction and control strategies for PV-bess integrated electric vehicle charging station. *Renew. Energy Focus*. **48**, 100523 (2024).
7. Mansouri, N. et al. Control and optimization of hydrogen hybrid electric vehicles using gps-based speed estimation. *Electronics* **14** (1), 110 (2024).
8. Ilahi, T. et al. Comprehensive design analysis of economical E-Bike charger with IoT-empowered system for real-time parameter monitoring. *J. Adv. Transp.* **2024** (1), 2387983 (2024).
9. Wang, Y., Wu, Y., Tang, Y., Li, Q. & He, H. Cooperative energy management and eco-driving of plug-in hybrid electric vehicle via multi-agent reinforcement learning. *Appl. Energy*. **332**, 120563 (2023).
10. Mansouri, N. et al. Reserve technique in integrating large sustainable energy sources: a case study of the Tunisian grid. *Sustainability* **16** (23), 10791 (2024).
11. Fathy, A. Bald eagle search optimizer-based energy management strategy for microgrid with renewable sources and electric vehicles. *Appl. Energy*. **334**, 120688 (2023).
12. Gulraiz, A. et al. Impact of photovoltaic ingress on the performance and stability of low voltage grid-connected microgrids. *Results Eng.* **2025**, 105030 (2025).
13. Chaurasia, K. & Ravishankar Kamath, H. Microgrid energy management using electric vehicles. In *Flexible Electronics for Electric Vehicles: Select Proceedings of FlexEV—2021. Oct 5:629 – 35* (2022).
14. Ali, M., Vasquez, J. C., Guerrero, J. M., Guan, Y. & Bazmohammadi, N. Microgrid an energy solution for remote islanded communities in Indonesia. In *2024 IEEE 10th International Power Electronics and Motion Control Conference (IPEMC2024-ECCE Asia)* 3799–3804 (IEEE, 2024).
15. Karami, M., Zadehbagheri, M., Kiani, M. J. & Nejatian, S. Retailer energy management of electric energy by combining demand response and hydrogen storage systems, renewable sources and electric vehicles. *Int. J. Hydrog. Energy*. **48** (49), 18775–18794 (2023).
16. Mazhar, T. et al. Electric vehicle charging system in the smart grid using different machine learning methods. *Sustainability* **15** (3), 2603 (2023).
17. Ali, M. et al. Microgrids for energy access in remote and islanded communities under natural disasters–Context of Lombok Island Indonesia. *Renew. Energy Focus* **2025**, 100705 (2025).
18. Karmaker, A. K., Hossain, M. A., Pota, H. R., Onen, A. & Jung, J. Energy management system for hybrid renewable energy-based electric vehicle charging station. *IEEE Access.* **11**, 27793–27805 (2023).
19. Hasani, R., Mohammadi, M. & Samanfar, A. Integrated multiobjective energy management for a smart microgrid incorporating electric vehicle charging stations and demand response programs under uncertainty. *Int. J. Energy Res.* **2025** (1), 9531493 (2025).
20. Engelhardt, J., Zepter, J. M., Gabderakhmanova, T. & Marinelli, M. Energy management of a multi-battery system for renewable-based high power EV charging. *ETransportation* **14**, 100198 (2022).
21. Mohamed, N., Aymen, F., Ali, Z. M., Zobaa, A. F. & Aleem, A. S.H., Efficient power management strategy of electric vehicles-based hybrid renewable energy. *Sustainability* **13** (13), 7351 (2021).
22. Mohan, H. M. & Dash, S. K. Renewable energy-based DC microgrid with hybrid energy management system supporting electric vehicle charging system. *Systems* **11** (6), 273 (2023).
23. AL-Dhaifallah, M., Ali, Z. M., Alanazi, M., Dadfar, S. & Fazaeli, M. H. An efficient short-term energy management system for a microgrid with renewable power generation and electric vehicles. *Neural Comput. Appl.* **33** (23), 16095–16111 (2021).
24. Koca, Y. B. Adaptive energy management with machine learning in hybrid PV-wind systems for electric vehicle charging stations. *Electr. Eng.* **107** (4), 4771–4782 (2025).
25. Sathyan, S., Pandi, V. R., Antony, A., Salkuti, S. R. & Sreekumar, P. ANN-based energy management system for PV-powered EV charging station with battery backup and vehicle to grid support. *Int. J. Green Energy*. **21** (6), 1279–1294 (2024).
26. Shen, Y., Xie, J., He, T., Yao, L. & Xiao, Y. CEEMD-fuzzy control energy management of hybrid energy storage systems in electric vehicles. *IEEE Trans. Energy Convers.* **39** (1), 555–566 (2023).
27. Kamel, O. M., Diab, A. A. Z., Mahmoud, M. M., Al-Sumaiti, A. S. & Sultan, H. M. Performance enhancement of an islanded microgrid with the support of electrical vehicle and STATCOM systems. *Energies* **16** (4), 1577 (2023).
28. Kamel, O. M., Abdelaziz, A. Y. & Zaki Diab, A. A. Damping oscillation techniques for wind farm DFIG integrated into inter-connected power system. *Electr. Power Compon. Syst.* **48** (14–15), 1551–1570 (2020).
29. yyah, A., Sozer, Y. & Elbuluk, M. E. Modeling and control design of microgrid-connected PV-based sources. *IEEE J. Emerg. Sel. Top. Power Electron.* **2**, 907–919 (2014).
30. Khorramabadi, S. & Bakhshai, A. Critic-based self-tuning PI structure for active and reactive power control of VSCs in microgrid systems. *IEEE Trans. Smart Grid*. **6**, 92–103 (2015).
31. Halima, N. B., Hadj, N. B., Chaieb, M. & Neji, R. Energy management of parallel hybrid electric vehicle based on fuzzy logic control strategies. *J. Circuits Syst. Comput.* **32** (01), 2350007 (2023).
32. Agushaka, J. O., Ezugwu, A. E. & Abualigah, L. Dwarf mongoose optimization algorithm. *Comput. Methods Appl. Mech. Eng.* **391**, 114570 (2022).

33. Givi, H., Dehghani, M. & Hubálovský, Š. Red panda optimization algorithm: an effective bio-inspired metaheuristic algorithm for solving engineering optimization problems. *IEEe Access.* **11**, 57203–57227 (2023).
34. Venkatesh, R. J., Priya, R., Hemachandu, P. & Reddy, C. V. K. An optimization approach control of EV solar charging system with step-up DC–DC converter. *Analog Integr. Circuits Signal Process.* **119** (2), 215–232 (2024).
35. Hsu, C. Y. et al. Power management in isolated microgrids using machine learning-based robust model predictive control. *Results Eng.* **27**, 106170 (2025).
36. Aeggegn, D. B., Nyakoe, G. N. & Wekesa, C. ANFIS-controlled boost and bidirectional Buck-Boost DC-DC converters for solar PV, fuel cell, and BESS-based microgrid application. *Int. Trans. Electr. Energy Syst.* **2024** (1), 6484369 (2024).
37. El Boujdaini, L., Mezrhab, A., Moussaoui, M. A., Jurado, F. & Vera, D. Sizing of a stand-alone PV–wind–battery–diesel hybrid energy system and optimal combination using a particle swarm optimization algorithm. *Electr. Eng.* **104** (5), 3339–3359 (2022).
38. Sudhapriya, K. & Jaisiva, S. Implementation of artificial intelligence techniques in electric vehicles for battery management system. *Int. J. Low-Carbon Technol.* **20** (1), 590–604 (2025).
39. Makram Kamel, O. et al. Effective energy management strategy with a novel design of fuzzy logic and JAYA-based controllers in isolated DC/AC microgrids: a comparative analysis. *Wind Eng.* **49** (1), 199–222 (2025).

Author contributions

Rathika Natarajan—Writing, review and editing the original draft and Visualization. Jaisiva Selvaraj—Supervision and Investigation. Shyam Daniel—Conceptualization. Tefera Mekonnen Azerefegn—Project administration, Data curation and Validation.

Competing interests

The authors declare no conflict of interest.

Additional information

Correspondence and requests for materials should be addressed to T.M.A.

Reprints and permissions information is available at www.nature.com/reprints.

Publisher's note Springer Nature remains neutral with regard to jurisdictional claims in published maps and institutional affiliations.